Cardiovascular Revascularization Medicine 20 (2019) 392–398

Contents lists available at ScienceDirect

Cardiovascular Revascularization Medicine

First Report of Edge Vascular Response at 12 Months of Magmaris, A Second-Generation Drug-Eluting Resorbable Magnesium Scaffold, Assessed by Grayscale Intravascular Ultrasound, Virtual Histology, and Optical Coherence Tomography. A Biosolve-II Trial Sub-Study

Alexandre Hideo-Kajita [a], Hector M. Garcia-Garcia [a,*], Michael Haude [b], Michael Joner [c], Jacques Koolen [d], Hüseyin Ince [e], Alexandre Abizaid [f], Ralph Toelg [g], Pedro A. Lemos [h], Clemens von Birgelen [i], Evald Høj Christiansen [j], William Wijns [k], Franz-Josef Neumann [l], Christoph Kaiser [m], Eric Eeckhout [n], Lim Soo Teik [o], Javier Escaned [p], Viana Azizi [a], Kayode O. Kuku [a], Yuichi Ozaki [a], Kazuhiro Dan [a], Ron Waksman [a]

[a] Interventional Cardiology Department, MedStar Washington Hospital Center, Washington, DC, USA
[b] Medical Clinic I, Städtische Kliniken Neuss, Lukaskrankenhaus GmbH, Neuss, Germany
[c] Deutsches Herzzentrum Muenchen und Deutsches Zentrum fuer Herz-Kreislaufforschung e.V., Munich, Germany
[d] Cardiologie, Catharina Ziekenhuis, Eindhoven, the Netherlands
[e] Vivantes Klinikum im Friedrichshain and Am Urban, Department of Cardiology, University of Rostock, Berlin, Germany
[f] Instituto Dante Pazzanese de Cardiologia, São Paulo, Brazil
[g] Herzzentrum Segeberger Kliniken, Henstedt-Ulzburg, Germany
[h] Instituto do Coração – HCFMUSP, Universidade de São Paulo, São Paulo, Brazil
[i] Department of Cardiology, Medisch Spectrum Twente, Thoraxcentrum Twente, Enschede, the Netherlands
[j] Department of Cardiology, Aarhus University Hospital, Aarhus, Denmark
[k] Cardiology Department, Cardiovascular Research Center Aalst, OLV Hospital, Aalst, Belgium
[l] Klinik fur Kardiologie und Angiologie II, Universitats-Herzzentrum Freiburg - Bad Krozingen, Bad Krozingen, Germany
[m] Department of Cardiology, University Hospital, Basel, Switzerland
[n] Department of Cardiology, Lausanne University Hospital, Lausanne, Switzerland
[o] Department of Cardiology, National Heart Center Singapore, Singapore, Singapore
[p] Department of Cardiology, Hospital Clinico San Carlos, Madrid, Spain

ARTICLE INFO

Article history:
Received 29 November 2018
Received in revised form 11 January 2019
Accepted 13 February 2019

Keywords:
Magmaris
Edge vascular response
Optical coherence tomography
Grayscale intravascular ultrasound
Virtual histology

ABSTRACT

Introduction and objective: The edge vascular response (EVR) remains unknown in second generation drug-eluting Resorbable Magnesium Scaffold (RMS), such as Magmaris. The aim of the study was to evaluate tissue modifications in the RMS edges over time, assessed by different invasive imaging modalities.
Methods: The patients treated with the device were assessed by optical coherence tomography (OCT), grayscale intravascular ultrasound (IVUS), and virtual histology IVUS at baseline and 12 months. The EVR study performed a segment- and frame-level analysis of the 5 mm segments proximal and distal of the actual RMS.
Results: The segment-level grayscale IVUS (n = 10), virtual histology IVUS (n = 10), and OCT (n = 18) analysis did not show any significant changes after 12 months, except for a fibrous plaque area (FPA) reduction of 0.5mm^2 ($p = 0.017$) in the proximal segment compared to baseline. In the frame-level analysis, IVUS evaluation revealed a vessel area decreased 2.80 ± 1.43 mm^2 ($p = 0.012$) and 2.49 ± 1.53 mm^2 ($p = 0.022$) in 2 proximal frames. This was accompanied by plaque area reduction of 0.88 ± 0.70 mm^2 ($p = 0.048$) and a FPA decreased by 0.63 ± 0.48 mm^2 ($p = 0.004$) in one proximal frame. In 1 distal frame, there was a dense calcium area reduction of 0.10 ± 0.12 mm^2 ($p = 0.045$), FPA and fibrous fatty plaque increased 0.54 ± 0.53 mm^2 ($p = 0.023$) and 0.17 ± 0.16 mm^2 ($p = 0.016$), respectively. By OCT, there was a lumen area decrease of 0.76 ± 1.51 mm^2 (p = 0.045) in a distal frame.
Conclusion: At 12 months, Magmaris EVR assessment does not show overall significant changes, except for a fibrous plaque area reduction in the proximal segment. This could be translated as a benign healing process at the edges of the RMS.
Summary: The edge vascular response (EVR) remains unknown in second generation drug-eluting absorbable metal scaffolds (RMS), such as Magmaris. Patients treated with the device were assessed by multi invasive

* Corresponding author at: Interventional Cardiology Department, MedStar Washington Hospital Center, 110 Irving St., NW, Suite 4B-1, Washington, DC 20010, USA.
E-mail address: hector.m.garciagarcia@medstar.net (H.M. Garcia-Garcia).

https://doi.org/10.1016/j.carrev.2019.02.019
1553-8389/

imaging modalities [i.e. optical coherence tomography (OCT), grayscale intravascular ultrasound (IVUS), and virtual histology IVUS] evaluating the tissue changes over time in the segment- and frame-level analysis of the 5 mm segments proximal and distal of the actual RMS. As a result, after 12 months, Magmaris EVR assessment does not show overall significant changes, except for a fibrous plaque area reduction in the proximal segment, translating a benign healing process at the edges of the RMS.

1. Background

The permanent metal encaging of the vessel wall promoted by the presence of bare metal stents (BMS) and drug-eluting stents (DES) in the coronary artery perpetuates inflammatory response and induces tissue changes at the stented segment including the proximal and distal device edges [1–8]. This phenomenon is denominated as edge vascular response (EVR). The EVR in metallic stents, BMS or DES (first and second generations), varies depending on the stent frame platform (polymer type and eluting-drug) [9–11]. For example, newer generation DES (i.e. second-generation and presumably more recent ones), EVR may present as luminal reduction at the proximal segment and positive remodeling of the vessel without luminal loss at the distal segment [11]. This occurrence, however, has not been described using second generation drug-eluting absorbable metal scaffolds, such as Magmaris (DREAMS-2G, Biotronik AG, Bülach, Switzerland) [12–15]. The aim of this study is to evaluate and compare the geometrical data and tissue composition of Magmaris EVR at baseline and 12-month follow-up using grayscale intravascular ultrasound (IVUS), virtual histology IVUS (VH-IVUS), and optical coherence tomography (OCT) [16,17].

2. Methods

The Biosolve II (NCT01960504) first-in-man trial details were described previously by Haude et al. [14,15]. In brief, Biosolve II was a multi-national, multi-center, single arm, non-randomized trial that enrolled 123 patients (n = 123 lesions) treated with Magmaris. The study population consisted of patients who were >18 years and <80 years old with either stable angina, unstable angina, or documented silent ischemia in the presence of de novo lesions with ≤21 mm in length and visually estimated percentage of diameter stenosis between >50% and ≤99%. The study excluded ostial lesion, bifurcation lesion, severe calcified lesion, arterial or venous graft on the target lesion, or rotation atherectomy. The EVR assessment of the device edges, proximal and distal segments (up to 5 mm each), was performed using grayscale IVUS, VH-IVUS, or OCT at baseline and after 12-month follow-up, comparing the differences between the phases (Fig. 1).

Grayscale IVUS and VH-IVUS images were attained by means of a 20 MHz catheter (Eagle Eye; Volcano Cooperation, Rancho Cordova, CA) or a 45 MHz catheter (Revolution; Volcano Cooperation, Rancho Cordova, CA). The OCT assessment was performed using frequency domain Ilumien system (St Jude Medical, Westford, MA, USA). The invasive imaging acquisition details were previously described elsewhere [15,16].

The different intravascular imaging methods were assessed at an independent core laboratory. The grayscale IVUS, VH-IVUS, and OCT baseline and the 12-month data evaluation were performed at Medstar Health Research Institute's Invasive coronary imaging Core Laboratory (Washington, DC, USA). The invasive imagining offline analysis was performed with dedicated software (QIVUS v3.0; MEDIS, Leiden, Netherlands) [16]. Grayscale IVUS assessments included the mean vessel, lumen, and plaque areas. VH-IVUS provided information on fibrous, fibrous-fatty, dense calcium and necrotic core areas [17]. The OCT analysis appraised the mean lumen area of every selected frame [18].

We performed a 2-level analysis. First, a segment level assessment of the entire 5 mm proximal or distal to the actual device edges, and second, a frame level evaluation of every 1 mm interval of each segment.

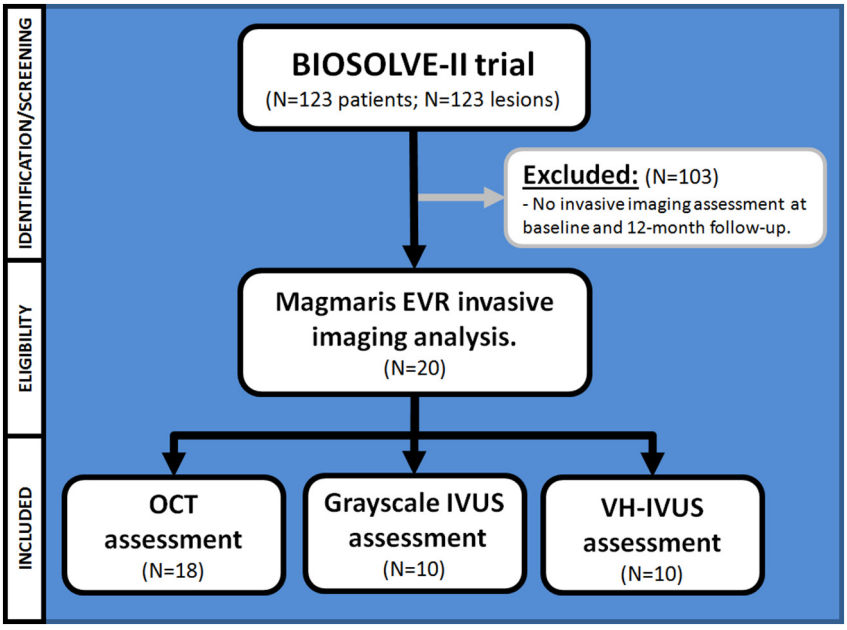

Fig. 1. Magmaris edge vascular response study flow diagram. Abbreviations: EVR = edges vascular response; IVUS = intravascular ultrasound; VH = virtual histology; OCT = optical coherence tomography.

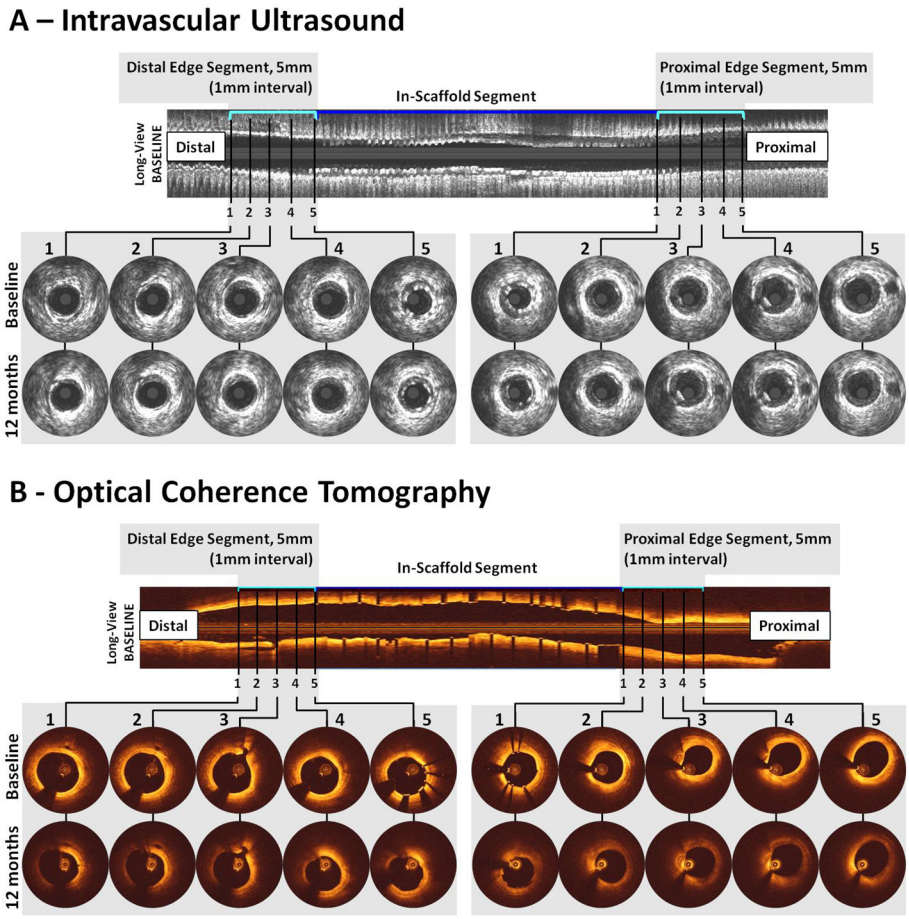

Fig. 2. Magmaris edge vascular response segment and frame level analysis panel. Intravascular ultrasound (A); and optical coherence tomography (B).

The segment level analysis data, for the proximal and distal device edges segment, were obtained by averaging the results of every 1 mm interval frame included in the frame level analysis. In the frame level analysis, the individual frames were labeled according to their position in the proximal or distal segments and were numbered 1 to 5 depending on the distance to device. Thus, proximal frame 1 and distal frame 5 were the closest frames to the scaffold edges. The selected frames in the segment and frame level analysis, at baseline and 12 months, were paired and matched for quantitative analysis (Fig. 2).

In the statistical analysis, the comparisons were tested using paired *t*-test. Results were considered significant at <0.05 level of significance. The products were presented using means and standard deviation. The analysis was performed using R-Statistics V.3.0 (R Foundation for Statistical Computing, Vienna, Austria) [19].

3. Results

Magmaris EVR invasive imaging analysis included 20 patients (n = 20 lesions) in the baseline to 12 months comparison (Fig. 1). Of whom, 10 lesions were assessed by grayscale IVUS and VH-IVUS, and 18 lesions were evaluated by OCT. The baseline characteristics are presented in Table 1. The study population mean age was 68.6 ± 9.6 years, 60% male patients, 75% stable angina, and 50% type B2 or C lesions. Lesion and procedural characteristics are shown in Table 2. The pre-procedure lesion length was 14.0 ± 4.0 mm, reference vessel diameter was 2.8 ± 0.3 mm, and the percentage of diameter stenosis was 54.7 ± 12.8% [by quantitative coronary angiography (QCA)]. All the target lesions were pre-dilated. The peri-procedure balloon diameter by artery diameter ratio was 1.04 ± 0.13, the scaffold diameter by artery diameter ratio was 1.1 ± 0.09, and the mean scaffold implantation pressure was 14.2 ± 2.2 atm. The post-procedure percentage of diameter stenosis in-scaffold and in-segment were 9.8 ± 6.8% and 17.8 ± 6.6%, respectively.

The segment level grayscale IVUS analysis did not reveal significant differences in mean vessel, lumen, or plaque areas in the proximal or distal segments after 12 months (Table 3). In the frame level assessment of the baseline to 12-month follow-up comparison, the mean vessel area reduced by 2.80 ± 1.43 mm^2 ($p = 0.012$) and by 2.49 ± 1.53 mm^2 ($p = 0.022$) in the proximal frames 4 and 5, respectively. There were no significant lumen area changes over time. The mean plaque area decreased 0.88 ± 0.70 mm^2 ($p = 0.048$) in the proximal frame 5 (Fig. 3).

In the segment level VH-IVUS analysis of the plaque composition, fibrous plaque area showed a mean reduction of 0.5 mm^2 ($p = 0.017$) in the proximal segment after 12 months. There were no statistically significant differences in fibrous plaque, fibrous fatty plaque, dense calcium, or necrotic core areas in the distal segment over time (Table 3). The frame level assessment of the fibrous plaque area revealed a reduction of 0.63 ± 0.48 mm^2 ($p = 0.004$) in the proximal frame 2 and an increase of 0.54 ± 0.53 mm^2 ($p = 0.023$) in the distal frame 4. The fibrous fatty plaque area incremented 0.17 ± 0.16 mm^2 ($p = 0.016$) in the distal frame 4, and dense calcium area decreased 0.10 ± 0.12 mm^2 ($p = 0.045$) in the distal frame 4 (Fig. 4).

The segment level OCT analysis of mean lumen area by OCT did not change in the baseline to 12-month follow-up comparison (Table 3). However, there was a significant reduction of mean lumen area in the frame level evaluation of 0.76 ± 1.51 mm^2 ($p = 0.045$) in the distal frame 2 after 12 months (Fig. 5).

Table 1
Baseline characteristics.

	Magmaris (N = 20)	
	N	%
Age, years (mean ± SD)	68.6	±9.6
Male gender	12	60.0
Risk factors		
History of hypertension	17	85.0
History of hypercholesterolemia	9	45.0
History of diabetes mellitus	5	25.0
History of smoking	9	45.0
History of myocardial infarction	5	25.0
Previous revascularization[a]	12	60.0
Clinical presentation		
Stable angina	15	75.0
Unstable angina	2	10.0
Silent ischemia	3	15.0
Medications		
ASA	20	100.0
Clopidogrel	20	100.0
Statins	16	80.0
Multi-vessel disease	20	100.0
Target vessel		
LMCA	0	0.0
LAD	8	40.0
LCx	5	25.0
RCA	7	35.0
ACC/AHA lesion classification		
Type A	1	5.0
Type B1	9	45.0
Type B2	8	40.0
Type C	2	10.0

Abbreviations: ACC = American College of Cardiology; AHA = American Heart Association; ASA = acetylsalicylic acid; CABG = coronary artery bypass graft; LAD = left anterior descending artery; LCx = left circumflex artery; LMCA = left main coronary artery; PCI = percutaneous coronary intervention; RCA = right coronary artery; SD = standard deviation.
[a] PCI or CABG.

Table 2
Lesion and procedural characteristics.

	Magmaris (N = 20)	
	Mean	±SD
Pre-procedure characteristics		
Lesion length, mm	14.0	±4.0
MLD, mm	1.3	±0.4
RVD, mm	2.8	±0.3
Pre-procedure %DS, %	54.7	±12.8
Peri-procedure characteristics		
Balloon pre-dilation		
Pre-dilation, N (%)	20	(100)
Diameter, mm	2.9	±0.2
Pre-dilation length, mm	12.8	±1.3
Pre-dilation balloon length/stent length ratio	0.61	±0.07
Balloon diameter/artery diameter ratio	1.04	±0.13
Scaffold		
Length, mm	21.0	±2.1
Diameter, mm	3.1	±0.2
MLD, mm	2.5	±0.3
Implantation pressure, atm	14.2	±2.2
Scaffold diameter/artery diameter ratio	1.1	±0.09
Balloon post-dilation		
Post-dilation balloon diameter, mm	3.2	±0.3
Post-dilation balloon length, mm	14.1	±4.5
Post-procedure characteristics		
In-stent		
MLD, mm	2.5	±0.3
RVD, mm	2.8	±0.3
%DS, %	9.8	±6.8
In-segment		
MLD, mm	2.3	±0.3
RVD, mm	2.7	±0.3
%DS, %	17.8	±6.6

Abbreviations: %DS = percentage of diameter stenosis; MLD = minimum lumen diameter; RVD = reference vessel diameter; SD = standard deviation.

Table 3
Magmaris edge vascular response *segment* level analysis in the Baseline to 12-month follow-up comparison assessed by grayscale IVUS, VH-IVUS and OCT.

	Grayscale IVUS				VH-IVUS				OCT
	Vessel Area, mm^2 (mean±SD)	Lumen Area, mm^2 (mean±SD)	Plaque Area, mm^2 (mean±SD)	Plaque Burden, % (mean±SD)	Fibrous plaque Area, mm^2 (mean±SD)	Fibrous Fatty Area, mm^2 (mean±SD)	Dense Area, mm^2 (mean±SD)	Necrotic Core Area, mm^2 (mean±SD)	Lumen Area, mm^2 (mean±SD)
Proximal	(N=9)				(N=9)				(N=17)
Baseline	15±2.8	7.6±2.4	7.5±1.0	50.6±8.0	2.6±0.7	0.4±0.2	0.5±0.4	1.0±0.3	7.8±2.8
12 months	14.3±2.2	7.2±2.0	7.1±1.0	50.5±7.0	2.1±0.7	0.3±0.2	0.6±0.3	0.9±0.4	7.7±2.9
p-value	0.390	0.550	0.270	0.960	0.017	0.14	0.180	0.480	0.840
Distal segment	(N=10)				(N=10)				(N=18)
Baseline	12.4±2.2	6.9±2.0	5.5±1.3	44.4±10.2	1.5±0.6	0.2±0.2	0.3±0.2	0.6±0.4	6.4±2.1
12 months	11.8±2.2	6.2±1.2	5.7±1.4	47.7±7.5	1.7±0.7	0.3±0.2	0.3±0.2	0.6±0.3	5.8±1.3
p-value	0.280	0.160	0.370	0.130	0.150	0.120	0.870	0.540	0.094

Abbreviations: IVUS = intravascular ultrasound; OCT = optical coherence tomography; VH = virtual histology; SD = standard deviation.

4. Discussion

The present study is the first report of Magmaris EVR assessed by grayscale IVUS, VH-IVUS, and OCT at 12 months. There are 3 main findings from our analysis: 1) The grayscale IVUS did not indicate any relevant changes in vessel, lumen, or plaque areas in the proximal or distal segments over time; albeit, there were considerable small vessel and plaque areas in 2 proximal and 1 proximal frames, respectively; 2) There was a noticeable decrease in fibrous plaque area in the proximal segment, a fibrous plaque area reduction in 1 proximal frame, and an increase of fibrous and fibrous fatty plaque areas with a decrease of dense calcium area in 1 distal frame; and 3) The luminal area by OCT did not change significantly in the proximal or distal frames or segments, except for a statistically relevant lumen area reduction in 1 distal frame.

The development of DES, first and second generations, reduced in-stent restenosis rates compared to bare metal stent-era results (i.e. 5–10%) and changed the in-stent restenosis pattern at the stented segment as well as at the device edges [11,20,21]. EVR in the DES era was heavily dictated by the differences in stent platforms, drugs, polymers, tissue composition, and geographical miss [10,11]. At the device edges, the vascular response in DES was known to be more intense (i.e. luminal reduction) in the proximal segment compared to the distal, most likely due to uncovered residual plaque (i.e. geographical miss) [11]. In contrast to previous published DES and bioresorbable vascular scaffold EVR data at 12 months, Magmaris EVR did not experience any relevant changes at the segment level although the frame level findings confirmed a reduction of mean plaque and vessel areas without any lumen area difference in the frame level analysis compared to baseline. Different than in metallic stents, Magmaris EVR can be partially explained by the fact that Magmaris promotes a transient scaffolding of the coronary vessel wall, avoiding the perpetuation of the inflammatory stimuli between baseline and 12 months, when >95% of the device struts were already absorbed.

The physiopathologic changes of the response-to-injury process at the stented segment and at the device edges of metallic and polymeric devices induces tissue composition alterations secondary to permanent or prolonged encaging of the vessel wall. Albeit, these changes are also determined by shear stress condition modifications in the treated segment and extensive vessel wall injury (e.g. intra-procedure instrumentation or spontaneous events) [11,20]. A serial invasive imaging study of the EVR changes, the BETAX trial, described a positive remodeling in

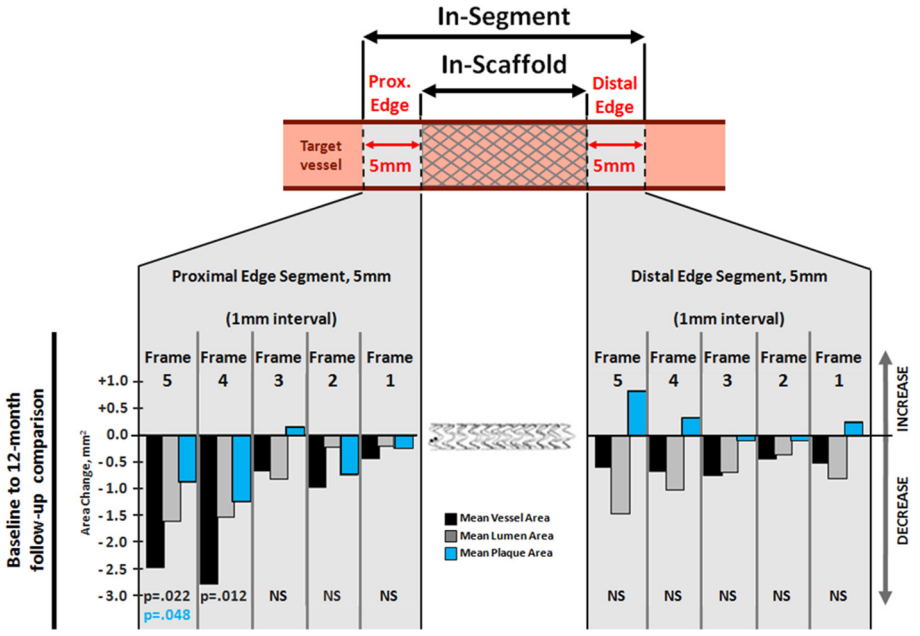

Fig. 3. Grayscale intravascular ultrasound *frame* level assessment of Magmaris edges vascular response in the baseline to 12-month follow-up comparison (mm^2). Abbreviations: NS = non-significant; Prox. = proximal.

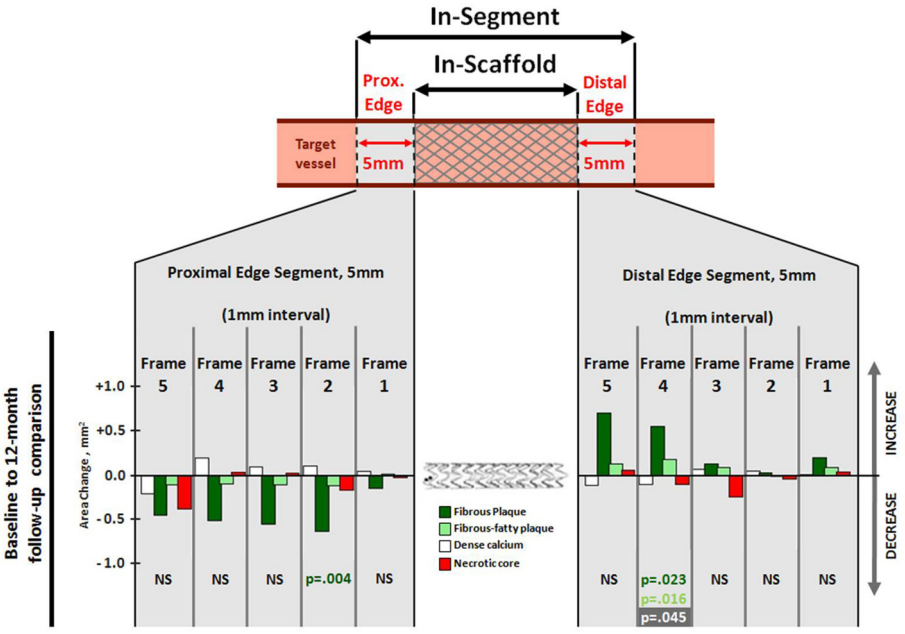

Fig. 4. Virtual histology-intravascular ultrasound *frame* level assessment of Magmaris edges vascular response in the Baseline to 12-month follow-up comparison (mm^2). Abbreviations: NS = non-significant; Prox. = proximal.

both edges at 6 months, mostly due to fibrous fatty plaque increase [10], which by VH-IVUS is associated to the presence of extracellular matrix, a neointimal growth factor [22–24]. Magmaris EVR tissue composition findings at 12 months showed a reduction of fibrous plaque area in the proximal segment. In the frame level comparison, there was a relevant increase of fibrous and fibrous fatty areas and a reduction of dense calcium area in 1 distal frame. Magmaris EVR at 12 months can be partially explained by careful peri-procedure implantation technique and a faster absorption time of the device, reducing the chronic inflammation process expressively over the stented segment and especially over the distal and proximal device edges [23,25].

Recently, the results reported by Zhang et al. in Absorb EVR assessed by OCT revealed a luminal area gain at 6 months followed by a significant luminal area decrease at 1, 2, and 3 years [26]. The luminal loss was present in the proximal and distal segments, particularly in the adjacent frames to the actual device edges [26]. On the other hand, Magmaris EVR segment level OCT findings did not show any relevant difference in lumen area over 12 months, albeit, the frame level comparison revealed an isolated but significant luminal area change in 1 distal frame in the same period of time, and not adjacent to Magmaris actual distal edge. It is true that Absorb and Magmaris are different in their very essence, but both are absorbable devices, which makes reasonable a parallel between the devices since Absorb takes, on average, at least 3 times as long as Magmaris to be absorbed. Magmaris EVR overall results at 6 and 12 months seem to be favorable compared to Absorb findings at 6 and 36 months.

The limitations apparent in the present study are listed as follows: 1) The present study was performed in a small cohort and therefore it was intended to be an exploratory analysis; 2) The number of patients

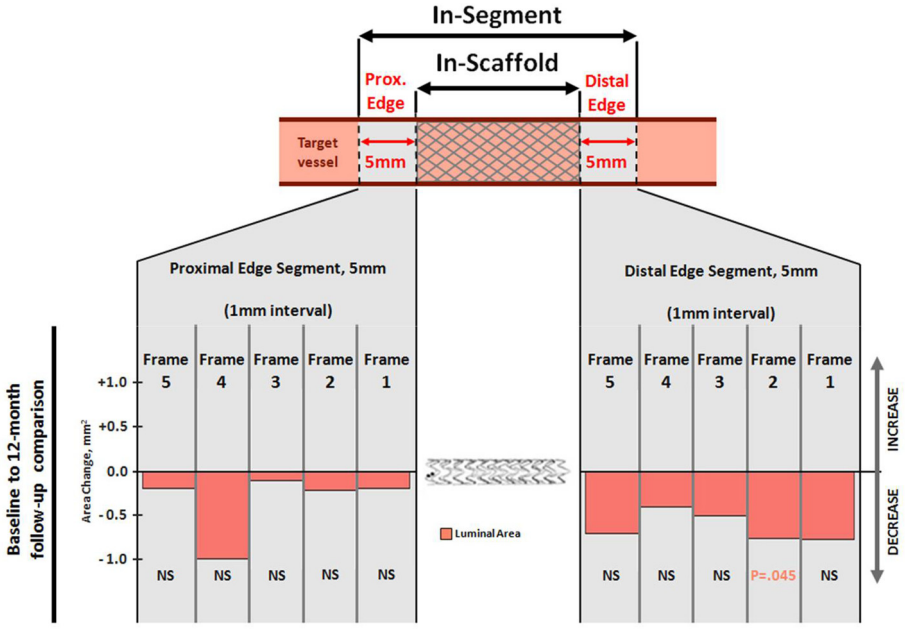

Fig. 5. Optical coherence tomography *frame* level assessment of Magmaris edges vascular response in the Baseline to 12-month follow-up comparison (mm^2). Abbreviations: NS = non-significant; Prox. = proximal.

assessed by grayscale and VH-IVUS was considerably lower than those evaluated by OCT; 3) Considering the mean absorption time of the Magmaris, there was no point to evaluate EVR after 1 year follow-up (95% of absorption); and 4) The tissue characterization between the edges and the in-scaffold segment was not performed in the 12 months analysis.

The transient scaffolding promoted by Magmaris (DREAMS 2G), assessed by grayscale IVUS, VH-IVUS, and OCT over a year did not present significant EVR changes in tissue composition and vessel, lumen, and plaque areas in the proximal or distal segments, except for a reduction in fibrous plaque area in the proximal segment.

References

[1] Sousa JE, Costa MA, Abizaid A, Abizaid AS, Feres F, Pinto IM, et al. Lack of neointimal proliferation after implantation of sirolimus-coated stents in human coronary arteries: a quantitative coronary angiography and three-dimensional intravascular ultrasound study. Circulation 2001;103:192–5.

[2] Morice MC, Serruys PW, Sousa JE, Fajadet J, Ban Hayashi E, Perin M, et al. A randomized comparison of a sirolimus-eluting stent with a standard stent for coronary revascularization. N Engl J Med 2002;346:1773–80.

[3] Ellis SG, Popma JJ, Lasala JM, Koglin JJ, Cox DA, Hermiller J, et al. Relationship between angiographic late loss and target lesion revascularization after coronary stent implantation: analysis from the TAXUS-IV trial. J Am Coll Cardiol 2005;45:1193–200.

[4] Serruys PW, Kutryk MJ, Ong AT. Coronary-artery stents. N Engl J Med 2006;354(5):483–95 [Review].

[5] Yoshizaki T, Naganuma T, Kobayashi T, Horikoshi T, Onishi H, Kawamoto H, et al. Long term follow-up of first generation versus new generation drug-eluting stents in three-vessel coronary artery disease. Cardiovasc Revasc Med 2017;18(7):492–6. https://doi.org/10.1016/j.carrev.2017.04.006.

[6] Subbotin VM. Analysis of arterial intimal hyperplasia: review and hypothesis. Theor Biol Med Model 2007;4:41. https://doi.org/10.1186/1742-4682-4-41.

[7] Finn AV, Joner M, Nakazawa G, Kolodgie F, Newell J, John MC, et al. Pathological correlates of late drug-eluting stent thrombosis: strut coverage as a marker of endothelialization. Circulation 2007;115:2435–41.

[8] Martí D, López E, Álvarez S, Palazuelos J, Rada I, Alfonso F. Neoatherosclerosis causing occlusive in-stent restenosis: impact of intracoronary imaging in the intensity of lipid-lowering therapy. Cardiovasc Revasc Med 2016;17(8):584–5. https://doi.org/10.1016/j.carrev.2016.09.013.

[9] Wakabayashi K, Waksman R, Weissman NJ. Edge effect from drug-eluting stents as assessed with serial intravascular ultrasound: a systematic review. Circ Cardiovasc Interv 2012;5(2):305–11. https://doi.org/10.1161/CIRCINTERVENTIONS.111.966259 [Review].

[10] García-García HM, Gonzalo N, Tanimoto S, Meliga E, de Jaegere P, Serruys PW. Characterization of edge effects with paclitaxel-eluting stents using serial intravascular ultrasound radiofrequency data analysis: the BETAX (BEside TAXus) study. Rev Esp Cardiol 2008;61(10):1013–9 [Erratum in: Rev Esp Cardiol. 2009; 62(4):463].

[11] Gogas BD, Garcia-Garcia HM, Onuma Y, Muramatsu T, Farooq V, Bourantas CV, et al. Edge vascular response after percutaneous coronary intervention: an intracoronary ultrasound and optical coherence tomography appraisal: from radioactive platforms to first- and second-generation drug-eluting stents and bioresorbable scaffolds. JACC Cardiovasc Interv 2013;6(3):211–21. https://doi.org/10.1016/j.jcin.2013.01.132 [Review].

[12] Campos CM, Muramatsu T, Iqbal J, Zhang YJ, Onuma Y, Garcia-Garcia HM, et al. Bioresorbable drug-eluting magnesium-alloy scaffold for treatment of coronary artery disease. Int J Mol Sci 2013;14(12):24492–500. https://doi.org/10.3390/ijms141224492.

[13] Iqbal J, Onuma Y, Ormiston J, Abizaid A, Waksman R, Serruys P. Bioresorbable scaffolds: rationale, current status, challenges, and future. Eur Heart J 2014;35:765–76.

[14] Haude M, Ince H, Abizaid A, Toelg R, Lemos PA, von Birgelen C, et al. Safety and performance of the second-generation drug-eluting absorbable metal scaffold in patients with de-novo coronary artery lesions (BIOSOLVE-II): 6 month results of a prospective, multicentre, non-randomised, first-in-man trial. Lancet 2016;387(10013):31–9. https://doi.org/10.1016/S0140-6736(15)00447-X.

[15] Haude M, Ince H, Abizaid A, Toelg R, Lemos PA, von Birgelen C, et al. Sustained safety and performance of the second-generation drug-eluting absorbable metal scaffold in patients with de novo coronary lesions: 12-month clinical results and angiographic findings of the BIOSOLVE-II first-in-man trial. Eur Heart J 2016;37(35):2701–9. https://doi.org/10.1093/eurheartj/ehw196.

[16] Garcia-Garcia HM, Haude M, Kuku K, Hideo-Kajita A, Ince H, Abizaid A, et al. In vivo serial invasive imaging of the second-generation drug-eluting absorbable metal scaffold (Magmaris - DREAMS 2G) in de novo coronary lesions: insights from the BIOSOLVE-II First-In-Man Trial. Int J Cardiol 2018 Mar 15;255:22–8. https://doi.org/10.1016/j.ijcard.2017.12.053.

[17] Mintz GS, Nissen SE, Anderson WD, Bailey SR, Erbel R, Fitzgerald PJ, et al. American College of Cardiology Clinical Expert Consensus Document on Standards for acquisition, measurement and reporting of intravascular ultrasound studies (IVUS). A report of the American College of Cardiology Task Force on Clinical Expert Consensus Documents. J Am Coll Cardiol 2001;37(5):1478–92.

[18] Tearney GJ, Regar E, Akasaka T, Adriaenssens T, Barlis P, Bezerra HG, et al. International Working Group for Intravascular Optical Coherence Tomography (IWG-IVOCT). Consensus standards for acquisition, measurement, and reporting of intravascular optical coherence tomography studies: a report from the International Working Group for Intravascular Optical Coherence Tomography Standardization and Validation. J Am Coll Cardiol 2012;59(12):1058–72. https://doi.org/10.1016/j.jacc.2011.09.079 [Erratum in: J Am Coll Cardiol. 2012; 59(18):1662. Dudeck, Darius [corrected to Dudek, Darius]; Falk, Erlin [corrected to Falk, Erling]; Garcia, Hector [corrected to Garcia-Garcia, Hector M]; Sonada, Shinjo [corrected to Sonoda, Shinjo]; Troels, Thim [corrected to Thim, Troels]; van Es, Gerrit-Ann [corrected to van Es, Gerrit-Anne]].

[19] R Core Team. R: A Language and Environment for Statistical Computing. Vienna, Austria: R Foundation for Statistical Computing; 2016 Available from: http://www.R-project.org/.

[20] Mehran R, Dangas G, Abizaid AS, Mintz GS, Lansky AJ, Satler LF, et al. Angiographic patterns of in-stent restenosis: classification and implications for long-term outcome. Circulation 1999;100(18):1872–8.

[21] Serruys PW, Degertekin M, Tanabe K, Russell ME, Guagliumi G, Webb J, et al. TAXUS II study group. Vascular responses at proximal and distal edges of paclitaxel-eluting stents: serial intravascular ultrasound analysis from the TAXUS II trial. Circulation 2004;109(5):627–33.

[22] Wentzel JJ, Gijsen FJ, Stergiopulos N, Serruys PW, Slager CJ, Krams R. Shear stress, vascular remodeling and neointimal formation. J Biomech 2003;36(5):681–8.

[23] Okada K, Honda Y, Kitahara H, Hollak MB, Yock PG, Popma JJ, et al. TCT-11 association between scaffold under-expansion and late lumen loss after bioresorbable scaffold implantation: IVUS and angiographic insights from the ABSORB Japan trial. J Am Coll Cardiol 2017;70(18) [suppl:B5].

[24] Farb A, Kolodgie FD, Hwang JY, Burke AP, Tefera K, Weber DK, et al. Extracellular matrix changes in stented human coronary arteries. Circulation 2004;110(8):940–7.

[25] Masiero G, Mojoli M, Barioli A, Paradies V, Cortese B, di Palma G, et al. TCT-9 absorb bioresorbable vascular scaffold vs. everolimus-eluting metallic stent in small vessel disease: a Propensity matched analysis of COMPARE II, RAI and MAASSTAD-ABSORB prospective studies. J Am Coll Cardiol 2017;70(18) [suppl:B4].

[26] Zhang YJ, Iqbal J, Nakatani S, Bourantas CV, Campos CM, Ishibashi Y, et al. ABSORB Cohort B Study Investigators. Scaffold and edge vascular response following implantation of everolimus-eluting bioresorbable vascular scaffold: a 3-year serial optical coherence tomography study. JACC Cardiovasc Interv 2014;7(12):1361–9. https://doi.org/10.1016/j.jcin.2014.06.025.